Supporting Information

External Stress-Free Reversible Multiple Shape Memory Polymers

Ya Nan Huang†, Long Fei Fan‡, Min Zhi Rong*†, Ming Qiu Zhang*†, and Yu Ming Gao¶*

†Key Laboratory for Polymeric Composite and Functional Materials of Ministry of Education, GD HPPC Lab, School of Chemistry, Sun Yat-Sen University, Guangzhou 510275, China

‡School of Textile Materials and Engineering, Wuyi University, Jiangmen, Guangdong 529020, China

¶Guangdong JISU New Materials Co., Ltd, Dongguan 523527, China

Author Information

Corresponding Authors

*E-mail: flf880221@163.com (L. F. Fan)

*E-mail: cesrmz@mail.sysu.edu.cn (M. Z. Rong)

*E-mail: ceszmq@mail.sysu.edu.cn (M. Q. Zhang)

Table S1. Typical multiple shape memory polymers

Polymers	SME			Switch mechanisms	Ref.
	One-way	Quasi two-way	True two-way		
Non-woven poly(ε-caprolactone) (PCL) fiber/epoxy-based copolymerthermoset system	●[a)]	○[b)]	○	Glass transition and melting	(S1)
Epoxy-based foam	●	○	○	Glass transition and melting	(S2)
PCL/poly(cyclohexyl methacrylate) (PCHMA) networks	●	○	○	Glass transition and melting	(S3)
PCL/PCHMA based nanocomposites	●	○	○	Glass transition and melting	S4)
Clay montmorillonite/PCL electrospun microfiber/epoxy composites	●	○	○	Glass transition and melting	(S5)
2-Dimethylamino-ethylmethacrylate (DMAEMA)/methyl-allyl-polyethenoxy-ether (TPEG) copolymer	●	○	○	Glass transition and melting	(S6)
Semicrystalline poly(decamethylene terephthalamide) (PA 10T)	●	○	○	Glass transition and melting	(S7)
Polyurethane (PU)/ethylene vinyl-acetate copolymer (EVA)/poly(vinyl acetate) (PVAc) multilayered films	●	○	○	Glass transition and melting	(S8)
Epoxy/PCL nanoweb	●	○	○	Glass transition and melting	(S9)
Commercial ethylene/1-butenecopolymer (TEPE)/carbon composites	●	○	○	Glass transition and melting	(S10)
Cellulose sisal fibre (SF)/PCL polyurethane networks	●	○	○	Glass transition and melting	(S11)
Poly(ester urethane)	●	○	○	Glass transition and melting	(S12)
Star-shaped polyhedral oligomeric silsesquioxane/poly(ε-caprolactone) polyurethane	●	○	○	Glass transition and melting	(S13)
Poly(ester urethane) (PBA3500)	●	○	○	Glass transition and melting	(S14)
PCL fiber/epoxy composites	●	○	○	Glass transition and melting	(S15)
PCL/epoxy	●	○	○	Glass transition	(S16)

				and melting	
Nanocrystalline non-isocyanate polyhydroxyurethanes	●	○	○	Glass transition and melting	(S17)
Poly(ether ether ketone) ionomer/sodium oleate composites	●	○	○	Glass transition and melting(	(S18)
Crosslinked poly(D,L-lactide) (PDLLA)/ poly(tetramethylene oxide) glycol (PTMEG) network	●	○	○	Glass transition and melting	(S19)
Poly(ethylene terephthalate) (PET) film	●	○	○	Glass transition and melting	(S20)
Poly(L-lactic acid)-b-poly(ethylene-co-butylene)-b-poly(L-lactic acid)	●	○	○	Glass transition and melting	(S21)
PCL/N,N-bis (2-hydroxyethyl) cinnamamide PU	●	○	○	Glass transition and melting	(S22)
4-Hexadecyloxybenzoic acid (HOBA)/shape-memory polyurethanes (SMPUs)	●	○	○	Glass transition and melting	(S23)
4-Hexadecyloxybenzoic acid (HOBA)/N,N-bis(2-hydroxylethyl) iso-nicotinamine (BINA) based PU complex	●	○	○	Glass transition and melting	(S24)
4,4-Azodibenzoic acid (Azoa)/hexamethylenediisocyanate (HDI)/PCL polyurethane networks	●	○	○	Glass transition and melting	(S25)
Lignin-co-poly(ester-amine-amide)	●	○	○	Two glass transitions	(S26)
Thiol−Michael addition based polymer networks	●	○	○	Two glass transitions	(S27)
Copolymer elastomers/clay nanocomposite	●	○	○	Two glass transitions	(S28)
Poly(propylene carbonate)/graphene oxide nanocomposites	●	○	○	Two glass transitions	(S29)
PU/PLA/PTMEG blends	●	○	○	Two glass transitions	(S30)
All-aromatic liquid crystal multiblock copoly(ether imide)s	●	○	○	Two glass transitions	(S31)
Silanized polyurethane/silane-functionalized graphene oxide nanocomposites bilayer	●	○	○	Two glass transitions	(S32)
Organic–inorganic nanocomposite bilayers	●	○	○	Two glass transitions	(S33)
Multicomposite styrene-based shape polymer	●	○	○	Two glass transitions	(S34)
Ethyl cellulose (EC)-g-tetrahydrofurfuryl methacrylate)-g-lauryl methacrylate polymers	●	○	○	Two glass transition	(S35)

PLA/PVAc/graphene nanocomposite blends	●	○	○	Two glass transitions	(S36)
Poly(mannitol sebacate)/electrospun poly(lactic acid) nanofibers composites	●	○	○	Two glass transitions	(S37)
SiO_2/epoxy resin nanocomposites	●	○	○	Two glass transitions	(S38)
epoxy bilayer polymer	●	○	○	Two glass transitions	(S39)
Peroxide crosslinked EVA/PCL blends	○	●	○	Two melting transitions	(S40)
Oligo(ω-pentadecalactone)/oligo(ε-caprolactone)/ oligotetrahydrofuran polymer network	●	○	○	Two melting transitions	(S41)
Star-shaped poly(ω-pentadecalactone) (PPD) and PCL copolymer network	●	○	○	Two melting transitions	(S42)
Star-shaped PPD/PCL copolymer	○	●	○	Two melting transitions	(S43)
PCL/PEG nanocomposites	●	○	○	Two melting transitions	(S44)
Silica-coated nanoparticles/PCL/PEG nanocomposites	●	○	○	Two melting transitions	(S45)
PCL/PEG copolymer network	●	○	○	Two melting transitions	(S46)
PCL-g-PEG network	●	○	○	Two melting transitions	(S47)
4-Octyldecyloxybenzoic acid (OOBA)/PEG-based SMPU	●	○	○	Two melting transitions	(S48)
4-Dodecyloxybenzoic acid/liquid-crystalline (LC) SMPU composites	●	○	○	Two melting transitions	(S49)
4-Hexadecyloxybenzoic acid (HOBA)-PEG based SMPU composites	●	○	○	Two melting transitions	(S50)
Supramolecular semicrystalline polyolefin elastomer blends	●	○	○	Two melting transitions	(S51)
Maleated-polystyrene-b-poly(ethylene-co-butylene)-b-polystyreneblock copolymer	●	○	○	Two melting transitions	(S52)
Crosslinked polyalkenamer based polymer blends	●	○	○	Two melting transitions	(S53)
Polyolefin elastomer/stearic acid composite	●	○	○	Two melting transitions	(S54)
Ionomer (Surlyn 9520)/polycyclooctene crosslinked polymer blends	●	○	○	Two melting transitions	(S55)
Crosslinked polyethylene/PCL blends	○	●	○	Two melting transitions	(S56)
Thermoplastic polyurethane/olefin block copolymer/polycaprolactone blends	●	○	○	Two melting transitions	(S57)

UPy-PTMEG/UPy-star shaped PCL network	●	○	○	Two melting transitions	(S58)
Poly(L-lactide)(PLA)/PCL/graphene nanoplatelets nanocomposite	●	○	○	Two melting transitions	(S59)
Silver nanowires/PCL blends	●	○	○	Two melting transitions	(S60)
Foamed eucommia ulmoides gum/high-density polyethylene (HDPE) composites	●	○	○	Two melting transitions	(S61)
Natural eucommia ulmoides rubber/polybutene-1 composites	●	○	○	Two melting transitions	(S62)
Crosslinked poly(ethylenevinyl acetate)/PCL blends	●	○	○	Two melting transitions	(S63)
Poly(tetramethylene oxide)/poly(p-dioxanone) co-network	●	○	○	Two melting transitions	(S64)
Poly(p-dioxanone)/PEG network	●	○	○	Two melting transitions	(S65)
UPy-functionalized PCL/poly(p-dioxanone) interpenetrating polymer networks (IPNs)	●	○	○	Two melting transitions	(S66)
Crosslinked polycyclooctene/carbon nanotube (CNT)/polyethylene nanocomposites	●	○	○	Two melting transitions	(S67)
Trans-1,4-polyisoprene (TPI)/low density polyethylene (LDPE) blends	●	○	○	Two melting transitions	(S68)
Semicrystalline ethylene-propylene-diene rubber/PCL blends	●	○	○	Two melting transitions	(S69)
PU/poly(methacrylic acid) (PMAA) network	●	○	○	Two melting transitions	(S70)
Crosslinked polyethylene (PE)/polypropylene(PP) blends	●	○	○	Two melting transitions	(S71)
Thermoplastic polyurethane (TPU)/poly(butylene succinate) (PBS)/PCL blends (SLBs) multilayers	●	○	○	Two melting transitions	(S72)
PCL/PTMEG polyurethane	●	○	○	Two melting transitions	(S73)
Cholesteryl isonicotinate/PCL based polyurethane	●	○	○	Two melting transitions	(S74)
4-n-Octyldecyloxybenzoic acid (OOBA)/pyridine-containing polyurethane complex	●	○	○	Two melting transitions	(S75)
Commercial UV curable glassy thermoset (Norland Optical Adhesive 63)	●	○	○	Broad glass transition	(S76)
Cellulose derivative	●	○	○	Broad glass transition	(S77)
α-Amino acid based poly(ester urea)s	●	○	○	Broad glass transition	(S78)
Crosslinked solution-polymerized styrene butadiene rubber	●	○	○	Broad glass transition	(S79)

Polyvinylpyrrolidone/poly(hydroxyethyl methacrylate-co-butyl acrylate) semi-IPNs	●	○	○	Broad glass transition	(S80)
PCL/poly(vinyl chloride) (PVC) blends	●	○	○	Broad glass transition	(S81)
A fluorine-containing difunctional benzoxazine	●	○	○	Broad glass transition	(S82)
Poly(methyl methacrylate) (PMMA)/PCL covalently crosslinked polymer co-network	●	○	○	Broad glass transition	(S83)
Poly(ester urea)s	●	○	○	Broad glass transition	(S84)
Epoxy based photo-curable resin with 3D printing method	●	○	○	Broad glass transition	(S85)
Poly(L-lactide) (PLLA)/PMMA blends	●	○	○	Broad glass transition	(S86)
UPy functionalized n-alkyl acrylate crosslinked network	●	○	○	Broad glass transition	(S87)
Nafion membrane	●	○	○	Broad glass transition	(S88)
HDPE/PEG thermoset polyurethane	●	○	○	Broad glass transition	(S89)
Perfluorosulphonic acid ionomer (PFSA)-Nafion	●	○	○	Broad glass transition	(S90)
Poly(benzoxazole-imide) (PIB)/polyetherimide (PIO) blends	●	○	○	Broad glass transition	(S91)
Carbon nanotube/water-borne epoxy nanocomposites	●	○	○	Broad glass transition	(S92)
ENR (a kind of epoxy)/$FeCl_3$ elastomer	●	○	○	Broad glass transition	(S93)
Bisphenol-A cyanate ester-bismaleimide crosslinked networks	●	○	○	Broad glass transition	(S94)
PU/PMMA composites	●	○	○	Broad glass transition	(S95)
Nafion	●	○	○	Broad glass transition	(S96)
Cholic acid-cinnamic acid-PEG crosslinked network	●	○	○	Broad glass transition	(S97)
2-Methoxyethyl acrylate-methylol acrylamide copolymer	●	○	○	Broad glass transition	(S98)
1,3-Adamantanediol-based polyurethanes	●	○	○	Broad glass transition	(S99)
3-Dimethyl (methacryloyloxyethyl)ammonium propane sulfonate-co-acrylic acid polymer	●	○	○	Broad glass transition	(S100)
Pyridine type zwitterionic polyurethane	●	○	○	Broad glass transition	(S101)

BINA/HDI/1,3-propanesultonezwitterionic polyurethanes	●	○	○	Broad glass transition	(S102)
Crosslinked poly[ethylene-co-(vinyl acetate)]	●	○	○	Broad melting transition	(S103)
Ethyl cellulose-g-PCL network	●	○	○	Broad melting transition	(S104)
Ethylene-1-octene copolymer (EOC)/LDPE/HDPE blends	●	○	○	Broad melting transition	(S105)
Paraffin/styrene-b-(ethylene-co-butylene)-b-styrene blends	●	○	○	Broad melting transition	(S106)
Star-shaped PCL based polyurethane	●	○	○	Broad melting transition	(S107)
Poly(vinyl alcohol)-g-polyurethane	●	○	○	Broad melting transition	(S108)
Side-chain liquid crystalline type random terpolymer networks	●	○	○	Glass transition and liquid crystal transition	(S109)
Side-chain liquid crystalline random terpolymers	●	○	○	Glass transition and liquid crystal transition	(S110)
Linear poly(lactic acid) (PLA) based copolymers	●	○	○	Glass transition and liquid crystal transition	(S111)
Liquid crystalline polyurethane networks	●	○	○	Glass transition and liquid crystal transition	(S112)
Side-chain liquid crystalline polyurethane networks	●	○	○	Glass transition and liquid crystal transition	(S113)
Liquid crystalline based poly(4-vinyl pyridine)	●	○	○	Glass transition and liquid crystal transition	(S114)
Polypropylene glycol-epoxy/PCL blends	●	○	○	Melting and glass transition	(S115)
Poly(cyclohexyl methacrylate)/PCL copolymer networks	●	○	○	Melting and glass transition	(S116)
Oligo(ε-caprolactone)dimethacrylate/silica coated magnetite nanoparticles nanocomposites	●	○	○	Narrow melting transition	(S117)
Polydopamine-poly(ε-caprolactone) network	●	○	○	Glass transition and a broad melting transition	(S118)
Polyurethane-based trilayer laminates	●	○	○	Three melting transitions	(S119)

Olefin block copolymer/ styrene-b-(ethylene-co-butylene)-b-styrene/paraffin blends	●	○	○	Three melting transitions	(S120)
Neat epoxy/p-aminodiphenylimide-epoxy /multiwalled carbon nanotube (MWCNT)-epoxy multicomposites	●	○	○	Melting and tran/cis photo-isomerization of azobenzene	(S121)
PMMA/PEG semi-interpenetrating networks (semi-IPNs)	●	○	○	Melting and broad glass transition	(S122)
Ethylene-1-octene copolymers (EOC)/HDPE/EOC blends	●	○	○	Multiple melting transitions	(S123)
PE/polycyclooctene blends	●	○	○	Multiple melting transitions	(S124)
PEG-4,4'-diphenylmethanediisocyanate (MDI)-dimethylol propionic acid (DMPA) polyurethane	●	○	○	Hydrogen bond and glass transition	(S125)
Epoxy network	●	○	○	Glass transition and Diels-Alder reaction	(S126)
$Zn(Mebip)_2(NTf_2)_2$/epoxy composites	●	○	○	Glass transition and metal complexes	(S127)
Spherical Fe_3O_4 nanoparticles/MWCNTs/epoxy nanocomposites	●	○	○	Multiple glass transitions	(S128)
Poly(L-lactide)/PTMEG copolymers	●	○	○	Melting and reversible photodimerization of anthracene groups	(S129)
4'-ethyoxy-4-(11-hydroxyundecyloxy)-azobenzene (EHAB)/GO nanocomposite films	●	○	○	Melting and trans/cis photo-isomerization of azobenzene	(S130)
This work	○	○	●	Two melting transitions	

[a]●:Applicable. [b]○: Not applicable.

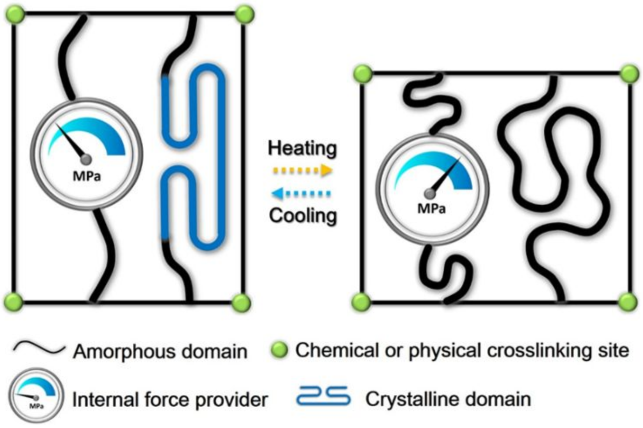

Figure S1. Schematic drawing of basic architecture of semi-crystalline two-way dual SMP capable of operating in the absence of external stress.

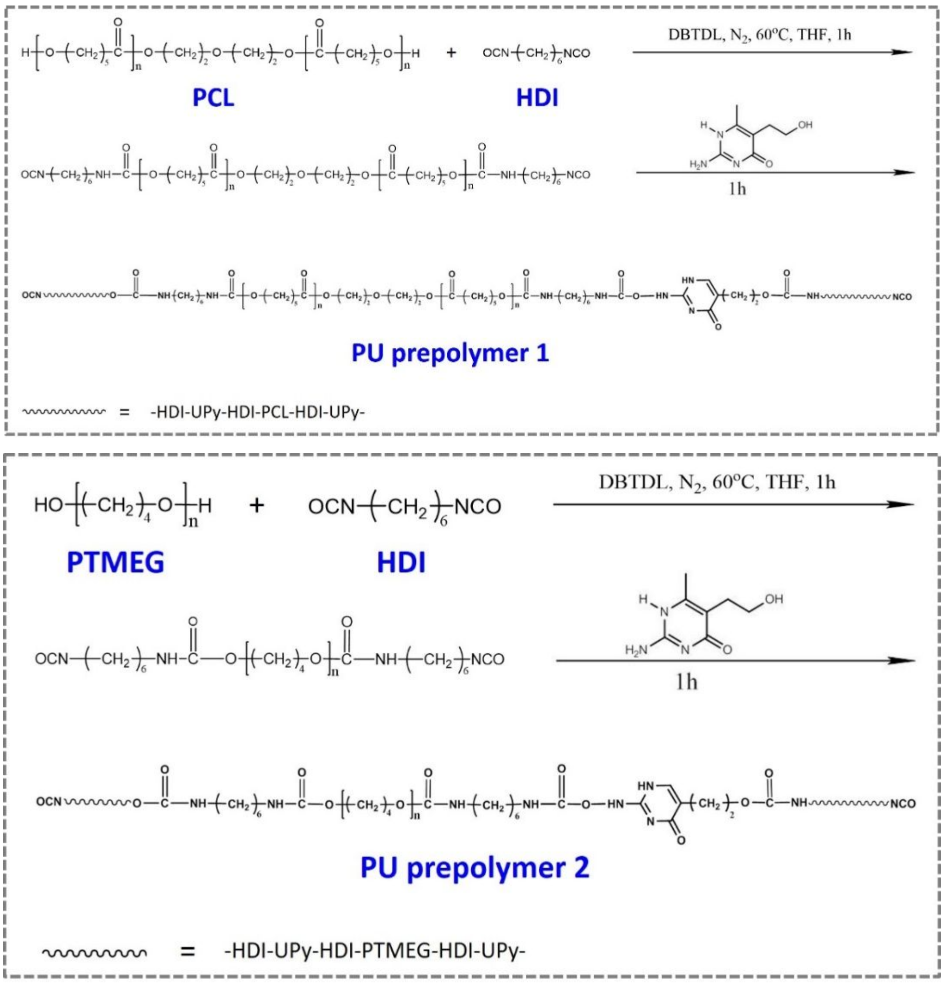

Figure S2. Synthesis of PU prepolymers.

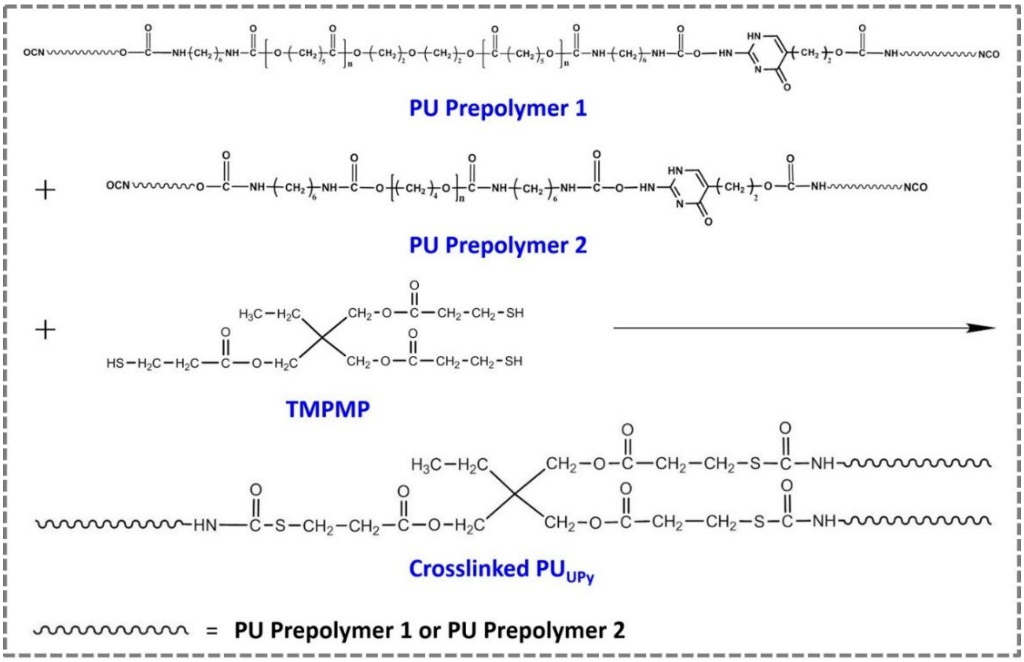

Figure S3. Crosslinking of PU prepolymers.

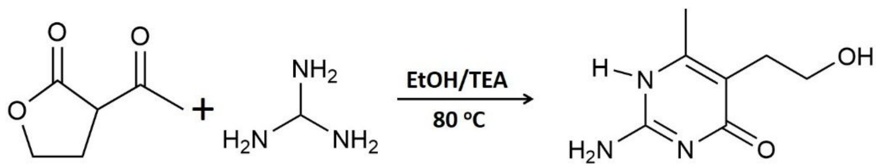

Figure S4. Synthesis of UPy.

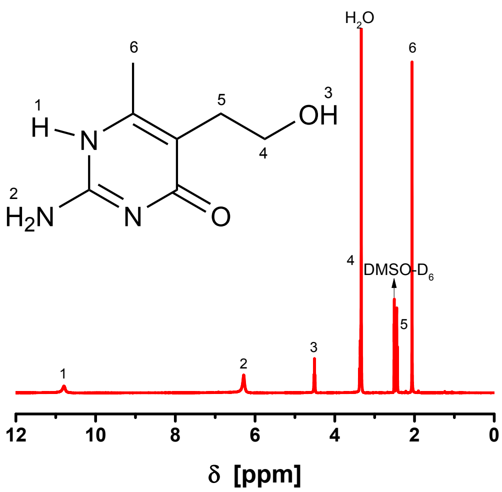

Figure S5. ^{1}H NMR spectra of UPy.

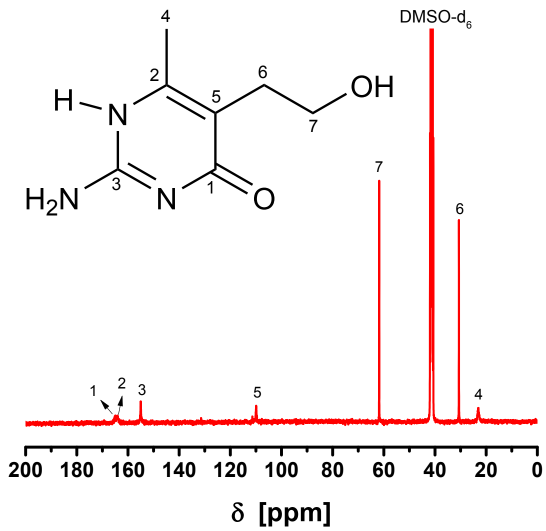

Figure S6. ^{13}C NMR spectrum of UPy.

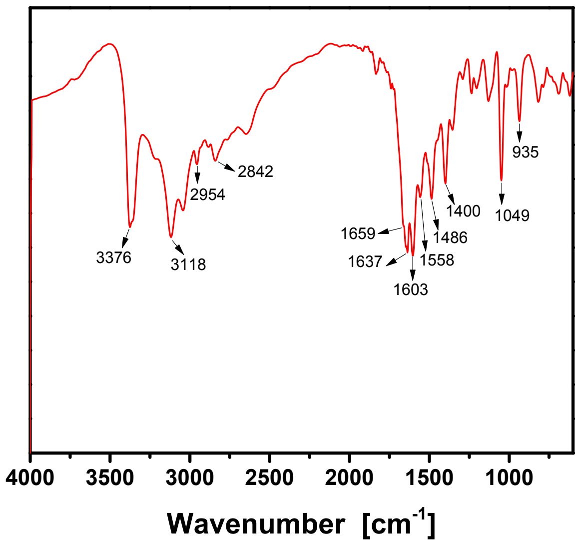

Figure S7. FTIR spectrum of UPy.

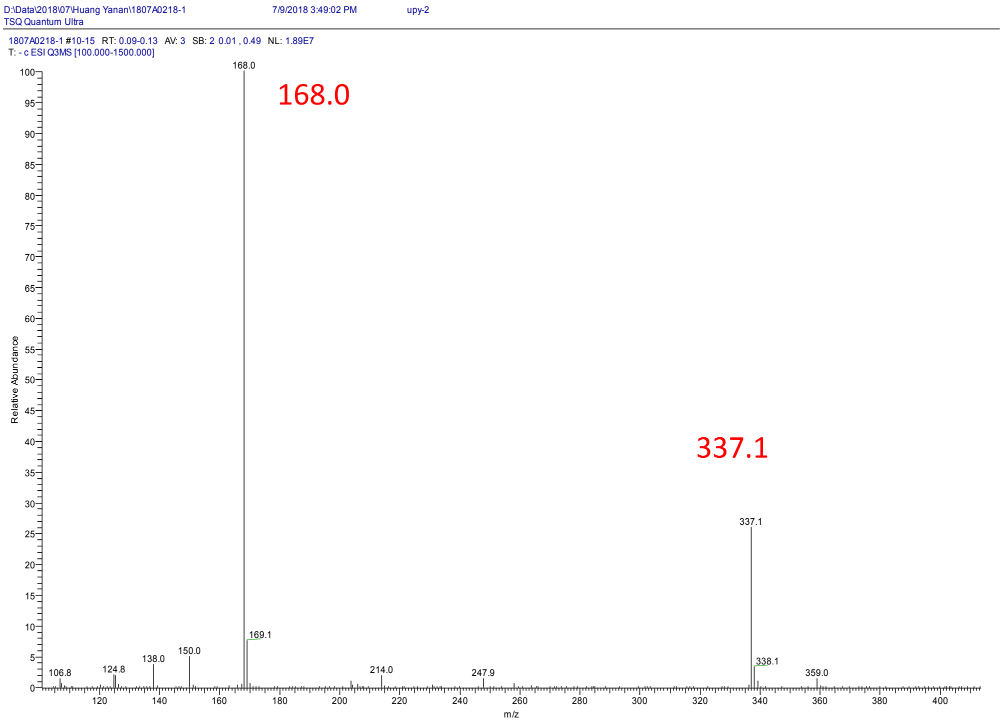

Figure S8. Mass spectrum of UPy.

Table S2. Effect of weight ratio of PCL/PTMEG on reversible strain of the programed PU_{UPy}

Formulae	PCL (g)	PTMEG (g)	HDI (g)	TMPMP (g)	UPy (g)	Average total reversible strain (%)	Reversible strain due to PCL segment (%)	Reversible strain due to PTMEG segment (%)
1#	3.00	26.10				9.26	-	-
2#	9.00	20.30				12.12	5.46	6.66
3#	15.00	14.50	3.70	1.91	0.81	10.75	8.77	1.98
4#	21.00	8.70				9.22	-	-
5#	27.00	2.90				7.88	-	-

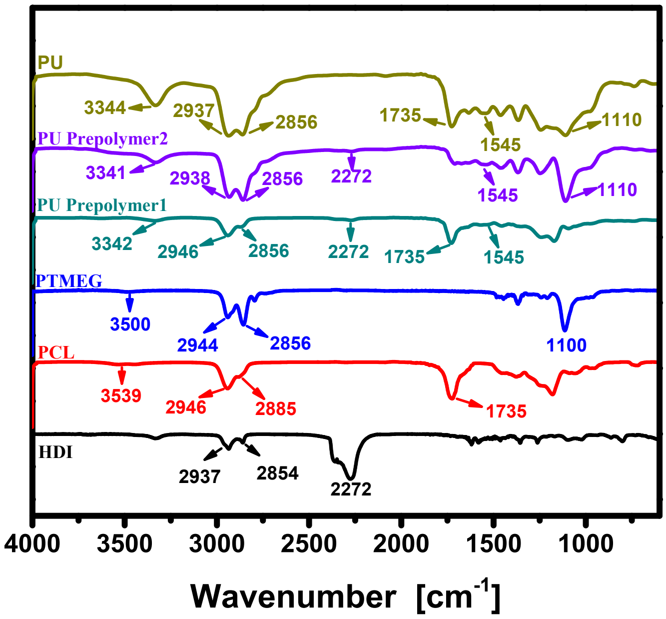

Figure S9. FTIR spectra of HDI, PCL, PTMEG, PU prepolymer 1, PU prepolymer 2, and PU_{UPy}. FTIR (KBr/cm^{-1}): HDI (2931, 2854 and 2272), PCL (3539, 2944, 2856 and 1735), PTMEG (3500, 2944, 2856 and 1100), PU prepolymer 1 (3342, 2946, 2856, 2272, 1735 and 1545), PU prepolymer 2 (3341, 2938, 2856, 2272, 1545 and 1110), and PU_{UPy} (3344, 2937, 2856, 1735, 1545 and 1110).

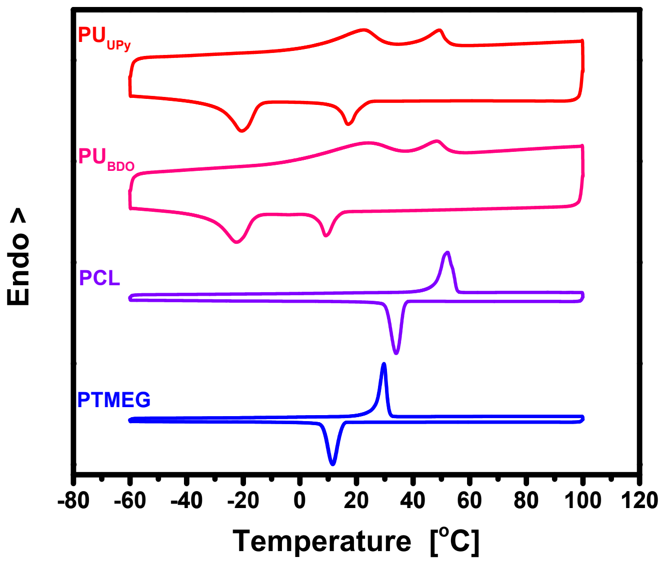

Figure S10. DSC heating and cooling scans of PU_{UPy}, PU_{BDO}, PCL and PTMEG (ramp: 3 °C/min).

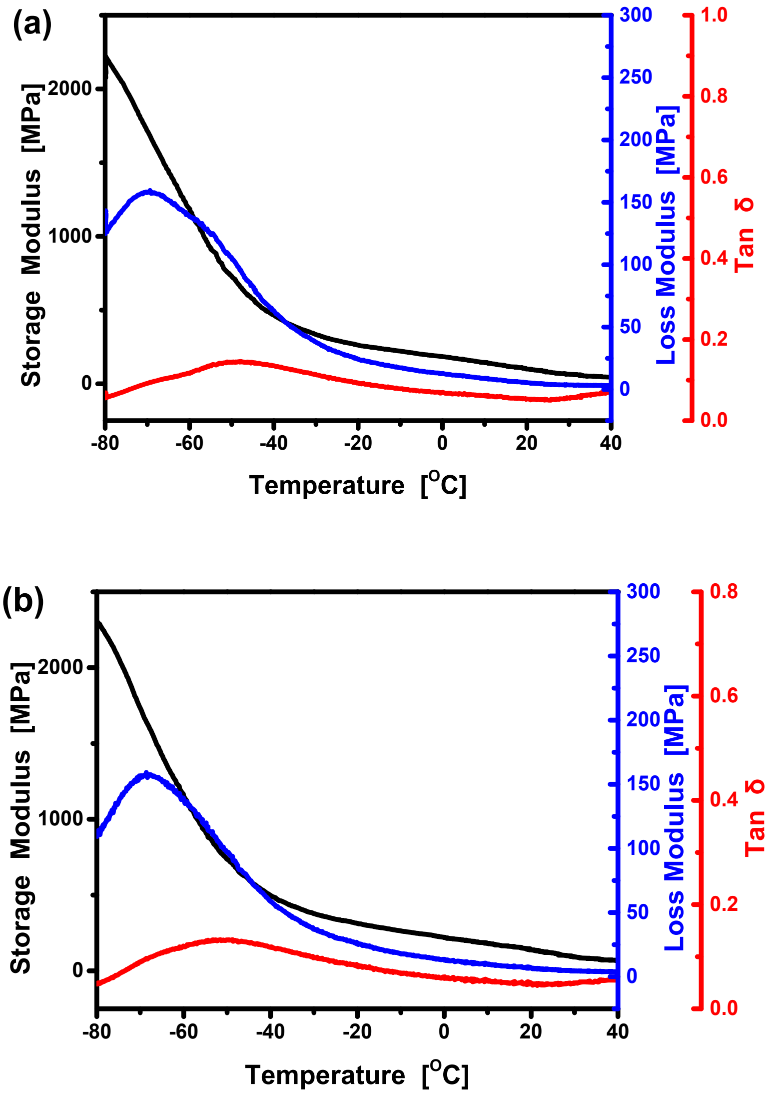

Figure S11. Typical DMA curves of (a) PU_{UPy} and (b) PU_{BDO} (ramp: 3 °C/min; frequency: 1 Hz). Note: The curves from 40 to 120 °C are not displayed because there is not any significant change within this range.

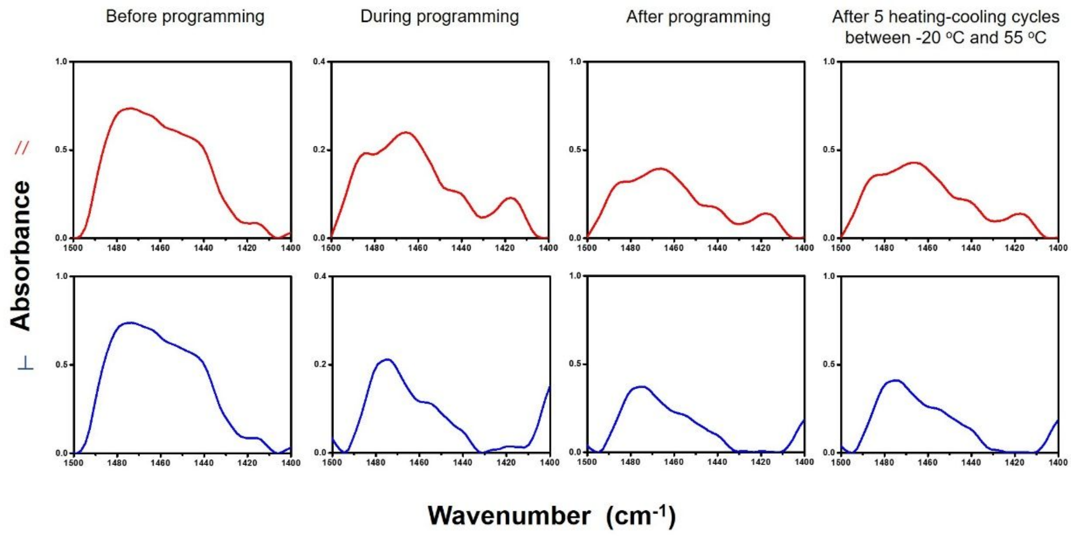

Figure S12. δ(-CH_2-) region on the FTIR spectra of the PU_{UPy} specimens. Note: The specimen measured during programming means that it was deformed to a temporary shape with strain of 400 % (refer to step ④ in **Figure 1**).

Table S3. Characterization of orientation of the PU_{UPy} specimen based on the measurement of FTIR dichroism in **Figure S12**

PU_{UPy}	Before programming	During programming*	After programming	After 5 heating-cooling cycles between -20 °C and 55 °C
$A_{//}$	0.68	0.68	0.67	0.62
$A_{\perp}$	0.68	0.46	0.53	0.50
R	1.00	1.49	1.26	1.24
(R-1)/(R+2)	0	0.14	0.08	0.07

*The specimen was deformed to a temporary shape with strain of 400 % (refer to step ④ in **Figure 1**).

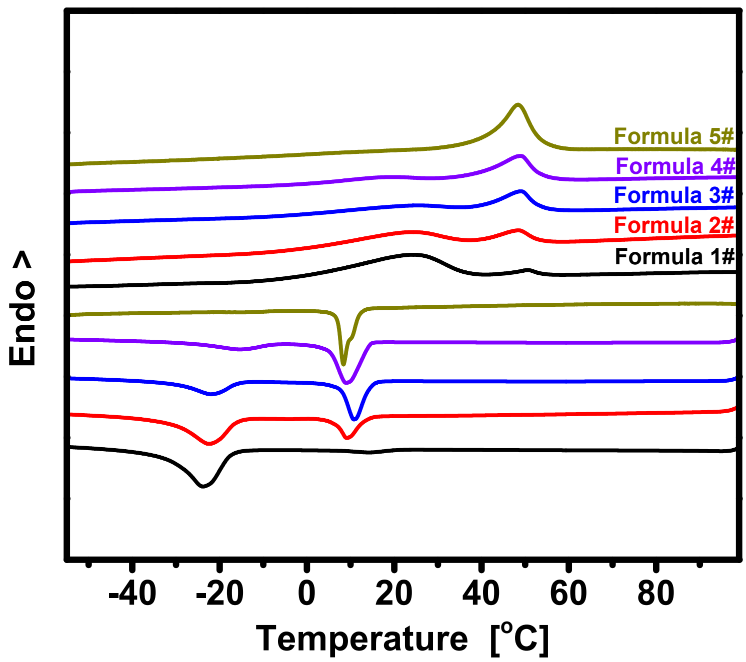

Figurer S13. DSC heating and cooling scans of the programmed PU_{UPy} (ramp: 3 °C/min).

Table S4. Characteristic parameters of the DSC curves of **Figure S13**

Formulae	PCL			PTMEG			Total X_c (%)
	T_m [a] (°C)	T_c [b] (°C)	X_c [c] (%)	T_m (°C)	T_c (°C)	X_c (%)	
PCL	51.14	34.48	61.20	-	-	-	-
PTMEG	-	-	-	29.80	11.60	55.04	-
1#	50.63	14.09	0.99	23.68	-23.89	18.22	19.21
2#	48.42	9.11	3.63	24.13	-22.44	9.08	12.71
3#	49.03	10.70	7.91	25.43	-21.97	4.61	12.52
4#	48.91	8.74	13.48	19.7	-15.32	2.93	16.41
5#	48.45	8.37	24.49	-	-14.62	0.24	24.73

[a] T_m: peak endothermic temperature; [b] T_c: peak exothermic temperature; [c] X_c: crystallinity of PTMEG or PCL calculated from $\Delta H_f/\Delta H_f^\circ$ (where ΔH_f denotes the measured heat of fusion, and ΔH_f° is the heat of fusion of 100 % crystalline PTMEG

(172.2 J g^{-1} [S131]) or PCL (139.5 J g^{-1} [S132])).

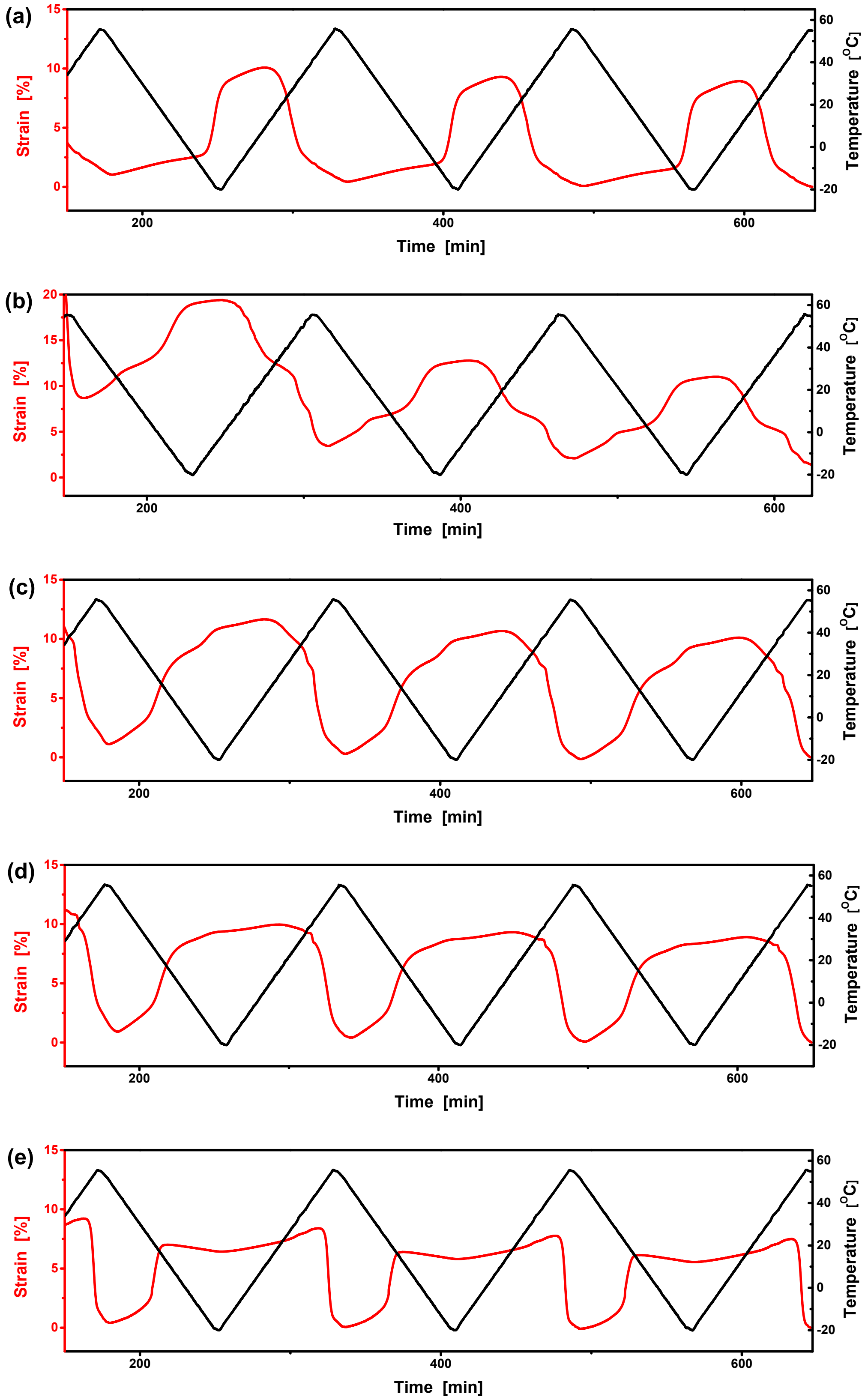

Figurer S14. Reversible strains measured by DMA of the programmed PU_{UPy} during repeated heating and cooling cycles between -20 and 55 °C (ramp: 3 °C/min). (a) Formula #1, (b) formula #2, (c) formula #3, (d) formula #4, and (e) formula #5.

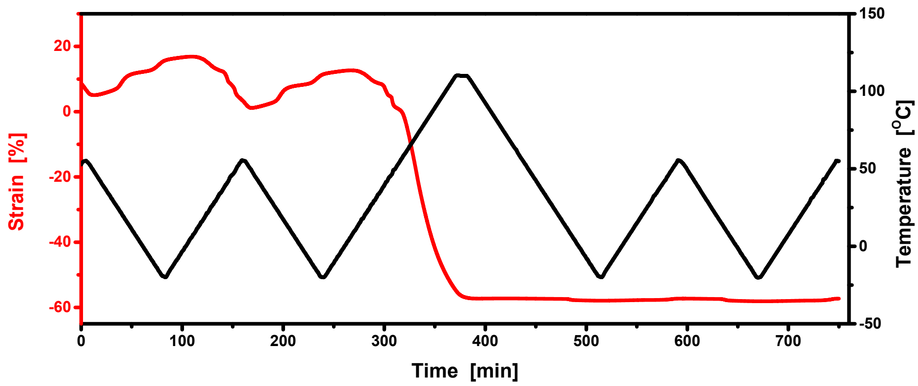

Figure S15. Thermomechanical behavior (measured by DMA) of the programmed PU_{UPy} before and after removing the internal stress provided by the hydrogen bonds.

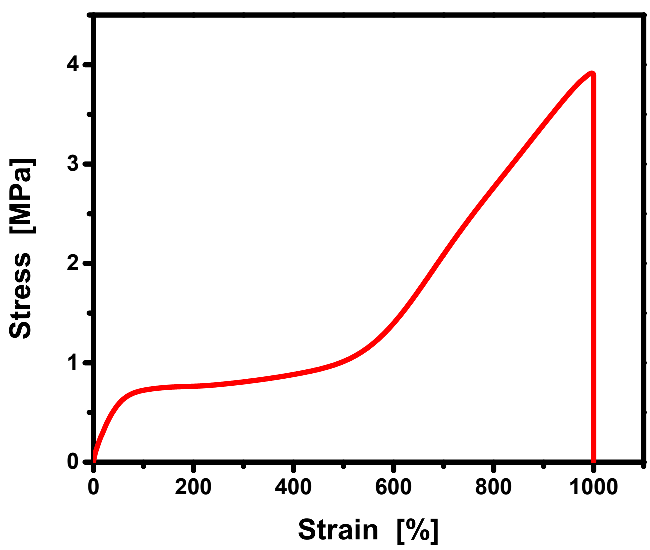

Figure S16. Typical tensile stress-strain curve of the PU_{UPy} measured at 49.1

°C. Prior to the test, the specimen was firstly immersed in the THF solution of LiBr (500 mL, 20 g/L) for 24 h at room temperature to remove the inter- and intra-macromolecular hydrogen bonds. Then, the specimen was dried at room temperature for 24 h allowing for evaporation of THF. Finally, the specimen was heated to 49.1 °C for 2 min and tested to failure under tension.

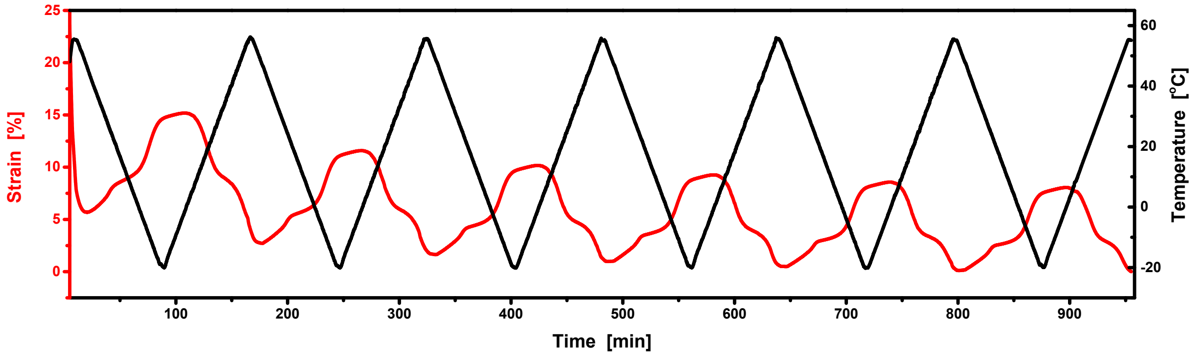

Figure 17. Thermomechanical behavior (measured by DMA) of the reprogrammed PU_{UPy} during repeated heating and cooling cycles between -20 and 55 °C (ramp: 1 °C/min). Note: The specimen used here was firstly programed and then lost its two-way shape memory effect by heating up to 110 ºC (**Figure S15**). Afterwards, it was reprogramed to obtained the two-way shape memory effect once again. The total average reversible strain of the reprogramed specimen is estimated to 10.5 % according to data collected during the first three heating/cooling cycles, and the average reversible strain induced by the melting of PCL and PTMEG are 4.8 % and 6.0 %, respectively. The results are close to those of the original programed version (**Figure 5b**).

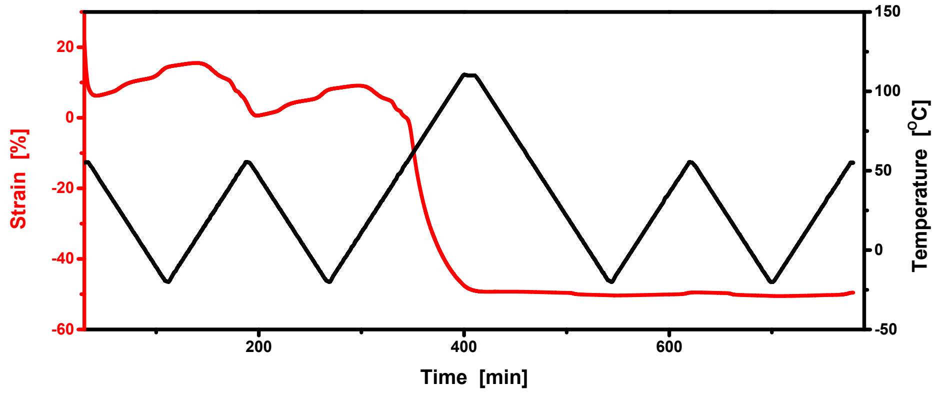

Figure S18. Thermomechanical behavior (measured by DMA) of the programmed PU_{BDO} before and after removing the internal stress provided by the hydrogen bonds.

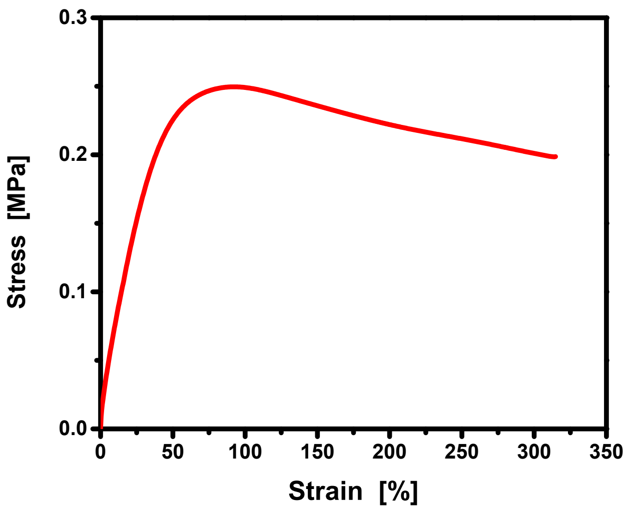

Figure S19. Typical tensile stress-strain curve of the PU_{BDO} measured at 47.7 °C. Prior to the test, the specimen was firstly immersed in the THF solution of

LiBr (500 mL, 20 g/L) for 24 h at room temperature to remove the inter- and intra-macromolecular hydrogen bonds. Then, the specimen was dried at room temperature for 24 h allowing for evaporation of THF. Finally, the specimen was heated to 47.7 °C for 2 min and tested to failure under tension.

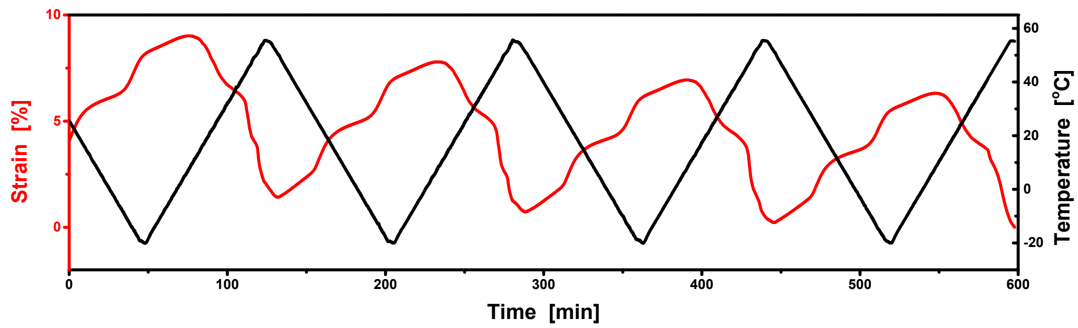

Figure S20. Thermomechanical behavior (measured by DMA) of the programmed PU_{BDO}. The first cycle that was used to remove the thermal history is not displayed for clarity.

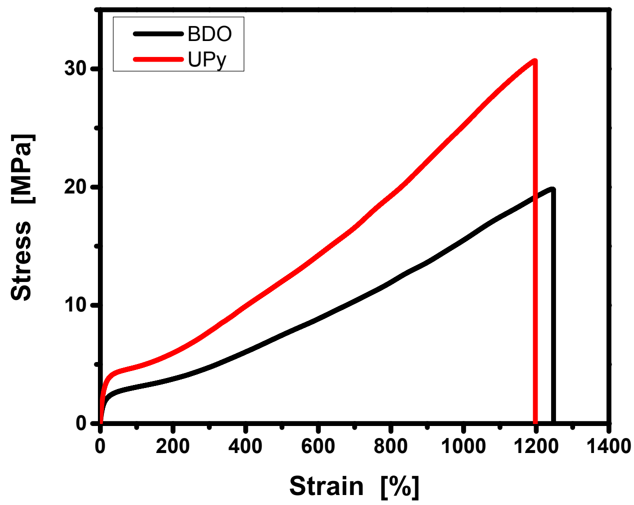

Figure S21. Typical tensile stress-strain curves of the programmed PU_{UPy} and PU_{BDO}.

Supporting references

(S1) Luo, X.; Mather, P. T. Triple-Shape Polymeric Composites (TSPCs). *Adv. Funct. Mater.* **2010**, *20*, 2649-2656.

(S2) Nejad, H. B.; Baker, R. M.; Mather, P. T. Preparation and Characterization of Triple Shape Memory Composite Foams. *Soft Matter* **2014**, *10*, 8066-8074.

(S3) Behl, M.; Bellin, I.; Kelch, S.; Wagermaier, W.; Lendlein, A. One-Step Process for Creating Triple-Shape Capability of AB Polymer Networks. *Adv. Funct. Mater.* **2009**, *19*, 102-108.

(S4) Kumar, U. N.; Kratz, K.; Wagermaier, W.; Behl, M.; Lendlein, A. Non-Contact Actuation of Triple-Shape Effect in Multiphase Polymer Network Nanocomposites in Alternating Magnetic Field. *J. Mater. Chem.* **2010**, *20*, 3404-3415.

(S5) Dong, Y.; Qian, C.; Lu, J.; Fu, Y. Clay Montmorillonite-Poly(e-caprolactone) Electrospun Microfiber/Epoxy Composites with Triple Shape Memory Effect. *Pigm. Resin Technol.* **2018**, *47*, 29-37.

(S6) Chen, Y.; Mo, F.; Chen, S.; Yang, Y.; Chen, S.; Zhuo, H.; Liu, J. A Shape Memory Copolymer Based on 2-(Dimethylamino)ethyl Methacrylate and Methyl Allyl Polyethenoxy Ether for Potential Biological Applications. *RSC Adv.* **2015**, *5*, 44435-44446.

(S7) Li, M.; Guan, Q.; Dingemans, T. J. High-Temperature Shape Memory Behavior of Semicrystalline Polyamide Thermosets. *ACS Appl. Mater. Interfaces* **2018**, *10*, 19106-19115.

(S8) Ji, S.; Wang, J.; Olah, A.; Baer, E. Triple-Shape-Memory Polymer Films Created by Forced-Assembly Multilayer Coextrusion. *J. Appl. Polym. Sci.* **2017**, *134*, 44405.

(S9) Fejos, M.; Molnar, K.; Karger-Kocsis, J. Epoxy/Polycaprolactone Systems with Triple-Shape Memory Effect: Electrospun Nanoweb with and without Graphene Versus Co-Continuous Morphology. *Materials* **2013**, *6*, 4489-4504.

(S10) Palza, H.; Zapata, P.; Sagredo, C. Shape Memory Composites Based on a Thermoplastic Elastomer Polyethylene with Carbon Nanostructures Stimulated by Heat and Solar Radiation Having Piezoresistive Behavior. *Polym. Int.* **2018**, *67*, 1046-1053.

(S11) Pan, L.; Xiong, Z.; Song, L.; Ban, J.; Lu, S. Synthesis and Characterization of Sisal Fibre Polyurethane Network Cross-Linked with Triple-Shape Memory Properties. *New J. Chem.* **2018**, *42*, 7130-7137.

(S12) Pretsch, T. Durability of a Polymer with Triple-Shape Properties. *Polym. Degrad. Stabil.* **2010**, *95*, 2515-2524.

(S13) Bothe, M.; Mya, K. Y.; Jie Lin, E. M.; Yeo, C. C.; Lu, X.; He, C.; Pretsch, T. Triple-Shape Properties of Star-Shaped POSS-Polycaprolactone Polyurethane Networks. *Soft Matter* **2012**, *8*, 965-972.

(S14) Pretsch, T. Triple-Shape Properties of a Thermoresponsive Poly(ester urethane). *Smart Mater. Struct.* **2010**, *19*, 015006.

(S15) Ge, Q.; Luo, X.; Iversen, C. B.; Mather, P. T.; Dunn, M. L.; Qi, H. J. Mechanisms of Triple-Shape Polymeric Composites Due to Dual Thermal Transitions. *Soft Matter* **2013**, *9*, 2212-2223.

(S16) Ge, Q.; Luo, X.; Iversen, C. B.; Nejad, H. B.; Mather, P. T.; Dunn, M. L.; Jerry Qi, H. A Finite Deformation Thermomechanical Constitutive Model for Triple

Shape Polymeric Composites Based on Dual Thermal Transitions. *Int. J. Solids Struct.* **2014**, *51*, 2777-2790.

(S17) Schimpf, V.; Heck, B.; Reiter, G.; Mülhaupt, R. Triple-Shape Memory Materials via Thermoresponsive Behavior of Nanocrystalline Non-Isocyanate Polyhydroxyurethanes. *Macromolecules* **2017**, *50*, 3598-3606.

(S18) Shi, Y.; Yoonessi, M.; Weiss, R. A. High Temperature Shape Memory Polymers. *Macromolecules* **2013**, *46*, 4160-4167.

(S19) Xie, H.; Cheng, C. Y.; Du, L.; Fan, C. J.; Deng, X. Y.; Yang, K. K.; Wang, Y. Z. A Facile Strategy To Construct PDLLA-PTMEG Network with Triple-Shape Effect via Photo-Cross-Linking of Anthracene Groups. *Macromolecules* **2016**, *49*, 3845-3855.

(S20) Wu, X. L.; Yang, C. P.; Guo, Y. Q.; Wang, H. Y. Triple-Shape Memory Effect in Poly (ethylene terephthalate) (PET) Film. *Pigm. Resin Technol.* **2018**, *47*, 55-62.

(S21) Zhou, J.; Cao, H.; Chang, R.; Shan, G.; Bao, Y.; Pan, P. Stereocomplexed and Homochiral Polyurethane Elastomers with Tunable Crystallizability and Multishape Memory Effects. *ACS Macro Lett.* **2018**, *7*, 233-238.

(S22) Wang, L.; Yang, X.; Chen, H.; Gong, T.; Li, W.; Yang, G.; Zhou, S. Design of Triple-Shape Memory Polyurethane with Photo-Cross-Linking of Cinnamon Groups. *ACS Appl. Mater. Interfaces* **2013**, *5*, 10520-10528.

(S23) Chen, S.; Yuan, H.; Ge, Z.; Chen, S.; Zhuo, H.; Liu, J. Insights into Liquid-Crystalline Shape-Memory Polyurethane Composites Based on an Amorphous Reversible Phase and Hexadecyloxybenzoic Acid. *J. Mater. Chem. C* **2014**, *2*, 1041-1049.

(S24) Chen, S.; Yuan, H.; Chen, S.; Yang, H.; Ge, Z.; Zhuo, H.; Liu, J. Development of Supramolecular Liquid-Crystalline Polyurethane Complexes Exhibiting Triple-Shape Functionality Using a One-Step Programming Process. *J. Mater. Chem. A* **2014**, *2*, 10169-10181.

(S25) Yang, J.; Wen, H.; Zhuo, H.; Chen, S.; Ban, J. A New Type of Photo-Thermo Staged-Responsive Shape-Memory Polyurethanes Network. *Polymers* **2017**, *9*, 287.

(S26) Sivasankarapillai, G.; Li, H.; McDonald, A. G. Lignin-Based Triple Shape Memory Polymers. *Biomacromolecules* **2015**, *16*, 2735-2742.

(S27) Chatani, S.; Wang, C.; Podgórski, M.; Bowman, C. N. Triple Shape Memory Materials Incorporating Two Distinct Polymer Networks Formed by Selective Thiol–Michael Addition Reactions. *Macromolecules* **2014**, *47*, 4949-4954.

(S28) Feng, X.; Zhang, G.; Zhuo, S.; Jiang, H.; Shi, J.; Li, F.; Li, H. Dual Responsive Shape Memory Polymer/Clay Nanocomposites. *Compos. Sci. Technol.* **2016**, *129*, 53-60.

(S29) Qi, X.; Guo, Y.; Wei, Y.; Dong, P.; Fu, Q. Multi-Shape and Temperature Memory Effects via Strong Physical Confinement in Poly(Propylene Carbonate)/Graphene Oxide Nanocomposites. *J. Phys. Chem. B* **2016**, *120*, 11064-11073.

(S30) Gu, S. Y.; Liu, L. L.; Gao, X. F. Triple-Shape Memory Properties of Polyurethane/Polylactide-Polytetramethylene Ether Blends. *Polym. Int.* **2015**, *64*, 1155-1162.

(S31) Guan, Q.; Picken, S. J.; Sheiko, S. S.; Dingemans, T. J. High-Temperature Shape Memory Behavior of Novel All-Aromatic (AB)n-Multiblock Copoly(ester imide)s. *Macromolecules* **2017**, *50*, 3903-3910.

(S32) Kim, Y. J.; Park, H. C.; Kim, B. K. Triple Shape-Memory Effect by Silanized Polyurethane/Silane-Functionalized Graphene Oxide Nanocomposites Bilayer. *High Perform. Polym.* **2015**, *27*, 886-897.

(S33) Bae, C. Y.; Park, J. H.; Kim, E. Y.; Kang, Y. S.; Kim, B. K. Organic–Inorganic Nanocomposite Bilayers with Triple Shape Memory Effect. *J. Mater. Chem.* **2011**, *21*, 11288-11295.

(S34) Li, W.; Liu, Y.; Leng, J. Selectively Actuated Multi-Shape Memory Effect of a Polymer Multicomposite. *J. Mater. Chem. A* **2015**, *3*, 24532-24539.

(S35) Lu, C.; Liu, Y.; Yu, J.; Wang, C.; Wang, J.; Chu, F. Fabrication of Well-Defined Shape Memory Graft Polymers Derived from Biomass: an Insight into the Effect of Side Chain Architecture on Shape Memory Properties. *Journal of Polymer Science Part A: Polym. Chem.* **2018**, *56*, 1711-1720.

(S36) Sabzi, M.; Babaahmadi, M.; Rahnama, M. Thermally and Electrically Triggered Triple-Shape Memory Behavior of Poly(vinyl acetate)/Poly(lactic acid) Due to Graphene-Induced Phase Separation. *ACS Appl. Mater. Interfaces* **2017**, *9*, 24061-24070.

(S37) Sonseca, Á.; Menes, O.; Giménez, E. A Comparative Study of the Mechanical, Shape-Memory, and Degradation Properties of Poly(lactic acid) Nanofiber and Cellulose Nanocrystal Reinforced Poly(mannitol sebacate) Nanocomposites. *RSC Adv.* **2017**, *7*, 21869-21882.

(S38) Li, X.; Zhu, Y.; Dong, Y.; Liu, M.; Ni, Q.; Fu, Y. Epoxy Resin Composite Bilayers with Triple-Shape Memory Effect. *J. Nanomater.* **2015**, *2015*, 1-8.

(S39) Xie, T.; Xiao, X.; Cheng, Y. T. Revealing Triple-Shape Memory Effect by Polymer Bilayers. *Macromol. Rapid Commun.* **2009**, *30*, 1823-1827.

(S40) Han, J.-L.; Lai, S.-M.; Chiu, Y. T. Two-Way Multi-Shape Memory Properties of Peroxide Crosslinked Ethylene Vinyl-Acetate Copolymer (EVA)/Polycaprolactone (PCL) Blends. *Polym. Adv. Technol.* **2018**, *29*, 2010-2024.

(S41) Nochel, U.; Behl, M.; Balk, M.; Lendlein, A. Thermally-Induced Triple-Shape Hydrogels: Soft Materials Enabling Complex Movements. *ACS Appl. Mater. Interfaces* **2016**, *8*, 28068-28076.

(S42) Zotzmann, J.; Behl, M.; Feng, Y.; Lendlein, A. Copolymer Networks Based on Poly(ω-pentadecalactone) and Poly(ϵ-caprolactone)Segments as a Versatile Triple-Shape Polymer System. *Adv. Funct. Mater.* **2010**, *20*, 3583-3594.

(S43) Zotzmann, J.; Behl, M.; Hofmann, D.; Lendlein, A. Reversible Triple-Shape Effect of Polymer Networks Containing Polypentadecalactone- and Poly(epsilon-caprolactone)-Segments. *Adv. Mater.* **2010**, *22*, 3424-3429.

(S44) Kumar, U. N.; Kratz, K.; Heuchel, M.; Behl, M.; Lendlein, A. Shape-Memory Nanocomposites with Magnetically Adjustable Apparent Switching Temperatures. *Adv. Mater.* **2011**, *23*, 4157-4162.

(S45) Narendra Kumar, U.; Kratz, K.; Behl, M.; Lendlein, A. Shape-Memory Properties of Magnetically Active Triple-Shape Nanocomposites Based on a Grafted Polymer Network with Two Crystallizable Switching Segments. *Express Polym. Lett.* **2012**, *6*, 26-40.

(S46) Bellin, I.; Kelch, S.; Lendlein, A. Dual-Shape Properties of Triple-Shape Polymer Networks with Crystallizable Network Segments and Grafted Side Chains. *J. Mater. Chem.* **2007**, *17*, 2885-2891.

(S47) Wagermaier, W.; Zander, T.; Hofmann, D.; Kratz, K.; Narendra Kumar, U.; Lendlein, A. In Situ X-Ray Scattering Studies of Poly(epsilon-caprolactone) Networks with Grafted Poly(ethylene glycol) Chains to Investigate Structural

Changes during Dual- and Triple-Shape Effect. *Macromol. Rapid Commun.* **2010**, *31*, 1546-1553.

(S48) Ban, J.; Zhu, L.; Chen, S.; Wang, Y. The Effect of 4-Octyldecyloxybenzoic Acid on Liquid-Crystalline Polyurethane Composites with Triple-Shape Memory and Self-Healing Properties. *Materials* **2016**, *9*, 792.

(S49) Ban, J.; Zhu, L.; Chen, S.; Wang, Y. The Impact of Liquid Crystal Fillers on Structure and Properties of Liquid-Crystalline Shape-Memory Polyurethane Composites I: 4-Dodecyloxybenzoic Acid. *J. Mater. Sci.* **2016**, *51*, 10229-10244.

(S50) Ban, J.; Zhu, L.; Chen, S.; Wang, Y. The Effect of Liquid Crystal Fillers on Structure and Properties of Liquid Crystalline Shape Memory Polyurethane Composites II: 4-Hexadecyloxybenzoic Acid. *J. Mater. Sci.* **2016**, *52*, 2628-2641.

(S51) Kashif, M.; Chang, Y. W. Supramolecular Semicrystalline Polyolefin Elastomer Blends with Triple-Shape Memory Effects. *Polym. Int.* **2016**, *65*, 577-583.

(S52) Suchao-in, K.; Chirachanchai, S. "Grafting to" as a Novel and Simple Approach for Triple-Shape Memory Polymers. *ACS Appl. Mater. Interfaces* **2013**, *5*, 6850-6853.

(S53) Cuevas, J. M.; Rubio, R.; Germán, L.; Laza, J. M.; Vilas, J. L.; Rodriguez, M.; León, L. M. Triple-Shape Memory Effect of Covalently Crosslinked Polyalkenamer Based Semicrystalline Polymer Blends. *Soft Matter* **2012**, *8*, 4928-4935.

(S54) Du, J.; Liu, D.; Zhang, Z.; Yao, X.; Wan, D.; Pu, H.; Lu, Z. Dual-Responsive Triple-Shape Memory Polyolefin Elastomer/Stearic Acid Composite. *Polymer* **2017**, *126*, 206-210.

(S55) García-Huete, N.; Post, W.; Laza, J. M.; Vilas, J. L.; León, L. M.; García, S. J. Effect of the Blend Ratio on the Shape Memory and Self-Healing Behaviour of

Ionomer-Polycyclooctene Crosslinked Polymer Blends. *Eur. Polym. J.* **2018**, *98*, 154-161.

(S56) Kolesov, I.; Dolynchuk, O.; Borreck, S.; Radusch, H. J. Morphology-Controlled Multiple One- and Two-Way Shape-Memory Behavior of Cross-Linked Polyethylene/Poly(ε-caprolactone) Blends. *Polym. Advan. Technol.* **2014**, *25*, 1315-1322.

(S57) Lai, S. M.; You, P.-Y.; Chiu, Y. T.; Kuo, C. W. Triple-Shape Memory Properties of Thermoplastic Polyurethane/Olefin Block Copolymer/Polycaprolactone Blends. *J. Polym. Res.* **2017**, *24,* 161-175.

(S58) Wei, M.; Zhan, M.; Yu, D.; Xie, H.; He, M.; Yang, K.; Wang, Y. Novel Poly(tetramethylene ether)Glycol and Poly(epsilon-caprolactone) Based Dynamic Network via Quadruple Hydrogen Bonding with Triple-Shape Effect and Self-Healing Capacity. *ACS Appl. Mater. Interfaces* **2015**, *7*, 2585-2596.

(S59) Khademeh Molavi, F.; Ghasemi, I.; Messori, M.; Esfandeh, M. Nanocomposites based on poly(l-lactide)/poly(ε-caprolactone) blends with Triple-Shape Memory Behavior: Effect of the Incorporation of Graphene Nanoplatelets (GNps). *Compos. Sci. Technol.* **2017**, *151*, 219-227.

(S60) Wang, H.; Luo, H.; Zhou, X.; Lin, Y.; Zhao, G.; Yi, G.; Cheng, X.; Wang, H.; Li, J. Conductive Multi-Shape Polymer Composites towards Stimuli Sensing. *Mater. Lett.* **2017**, *198*, 132-135.

(S61) Wang, Y.; Xia, L.; Xin, Z. Triple Shape Memory Effect of Foamed Natural Eucommia Ulmoides Gum/High-Density Polyethylene Composites. *Polym. Advan. Technol.* **2018**, *29*, 190-197.

(S62) Wang, Y.; Geng, J.; Xia, L.; Xin, Z. Multiple Shape Memory Behaviors of Natural Eucommia Ulmoides Rubber and Polybutene-1 Composites. *Polym. Int.* **2018**, *67*, 901-908.

(S63) Zhang, Z.X.; Wei, X.; Yang, J. H.; Zhang, N.; Huang, T.; Wang, Y.; Gao, X. L. Triple-Shape Memory Materials Based on Cross-Linked Poly(ethylene vinyl acetate) and Poly(ε-caprolactone). *Ind. Eng. Chem. Res.* **2016**, *55*, 12232-12241.

(S64) Zhang, J.; Niu, Y.; Huang, C.; Xiao, L.; Chen, Z.; Yang, K.; Wang, Y. Self-Healable and Recyclable Triple-Shape PPDO–PTMEG Co-Network Constructed through Thermoreversible Diels–Alder Reaction. *Polym. Chem.* **2012**, *3*, 1390-1393.

(S65) Niu, Y.; Zhang, P.; Zhang, J.; Xiao, L.; Yang, K.; Wang, Y. Poly(p-dioxanone)–Poly(ethylene glycol) Network: Synthesis, Characterization, and Its Shape Memory Effect. *Polym. Chem.* **2012**, *3*, 2508-2516.

(S66) Xiao, L.; Wei, M.; Zhan, M.; Zhang, J.; Xie, H.; Deng, X.; Yang, K.; Wang, Y. Novel Triple-Shape PCU/PPDO Interpenetrating Polymer Networks Constructed by Self-Complementary Quadruple Hydrogen Bonding and Covalent Bonding. *Polym. Chem.* **2014**, *5*, 2231-2241.

(S67) Wang, Z.; Zhao, J.; Chen, M.; Yang, M.; Tang, L.; Dang, Z. M.; Chen, F.; Huang, M.; Dong, X. Dually Actuated Triple Shape Memory Polymers of Cross-Linked Polycyclooctene-Carbon Nanotube/Polyethylene Nanocomposites. *ACS Appl. Mater. Interfaces* **2014**, *6*, 20051-20059.

(S68) Xia, L.; Xian, J.; Geng, J.; Wang, Y.; Shi, F.; Zhou, Z.; Lu, N.; Du, A.; Xin, Z. Multiple Shape Memory Effects of Trans-1,4-Polyisoprene and Low-Density Polyethylene Blends. *Polym. Int.* **2017**, *66*, 1382-1388.

(S69) Kashif, M.; Chang, Y.-W. Triple-Shape Memory Effects of Modified Semicrystalline Ethylene–Propylene–Diene Rubber/Poly(ε-caprolactone) Blends. *Eur. Polym. J.* **2015**, *70*, 306-316.

(S70) Zhang, Y.; Jiang, X.; Wu, R.; Wang, W. Multi-Stimuli Responsive Shape Memory Polymers Synthesized by Using Reaction-Induced Phase Separation. *J. Appl. Polym. Sci.* **2016**, *133*, 43534.

(S71) Zhao, J.; Chen, M.; Wang, X.; Zhao, X.; Wang, Z.; Dang, Z. M.; Ma, L.; Hu, G. H.; Chen, F. Triple Shape Memory Effects of Cross-Linked Polyethylene/Polypropylene Blends with Cocontinuous Architecture. *ACS Appl. Mater. Interfaces* **2013**, *5*, 5550-5556.

(S72) Zheng, Y.; Ji, X.; Yin, M.; Shen, J.; Guo, S. Strategy for Fabricating Multiple-Shape-Memory Polymeric Materials via the Multilayer Assembly of Co-Continuous Blends. *ACS Appl. Mater. Interfaces* **2017**, *9*, 32270-32279.

(S73) Chen, S.; Hu, J.; Yuen, C.-W.; Chan, L.; Zhuo, H. Triple Shape Memory Effect in Multiple Crystalline Polyurethanes. *Polym. Advan. Technol.* **2010**, *21*, 377-380.

(S74) Chen, H.; Liu, Y.; Gong, T.; Wang, L.; Zhao, K.; Zhou, S. Use of Intermolecular Hydrogen Bonding to Synthesize Triple-Shape Memory Supermolecular Composites. *RSC Adv.* **2013**, *3*, 7048-7056.

(S75) Chen, S.; Mo, F.; Chen, S.; Ge, Z.; Yang, H.; Zuo, J.; Liu, X.; Zhuo, H. New Insights into Multi-Shape Memory Behaviours and Liquid Crystalline Properties of Supramolecular Polyurethane Complexes Based on Pyridine-Containing Polyurethane and 4-Octyldecyloxybenzoic Acid. *J. Mater. Chem. A* **2015**, *3*, 19525-19538.

(S76) DiOrio, A. M.; Luo, X.; Lee, K. M.; Mather, P. T. A Functionally Graded Shape Memory Polymer. *Soft Matter* **2011**, *7*, 68-74.

(S77) Bai, Y.; Liu, Y.; Wang, Q. Cellulose Acetate for Shape Memory Polymer: Natural, Simple, High Performance, and Recyclable. *Adv. Polym. Tech.* **2018**, *37*, 869-877.

(S78) Peterson, G. I.; Dobrynin, A. V.; Becker, M. L. α-Amino Acid-Based Poly(Ester urea)s as Multishape Memory Polymers for Biomedical Applications. *ACS Macro Lett.* **2016**, *5*, 1176-1179.

(S79) Huang, J.; Zhang, L.; Tang, Z.; Wu, S.; Ning, N.; Sun, H.; Guo, B. Bioinspired Design of a Robust Elastomer with Adaptive Recovery via Triazolinedione Click Chemistry. *Macromol. Rapid Commun.* **2017**, *38*, 1600678.

(S80) Jiang, Z. C.; Xiao, Y. Y.; Kang, Y.; Li, B. J.; Zhang, S. Semi-IPNs with Moisture-Triggered Shape Memory and Self-Healing Properties. *Macromol. Rapid Commun.* **2017**, *38*, 1700149.

(S81) Liu, W.; Zhang, R.; Huang, M.; Dong, X.; Xu, W.; Ray, N.; Zhu, J. Design and Structural Study of a Triple-Shape Memory PCL/PVC Blend. *Polymer* **2016**, *104*, 115-122.

(S82) Liu, Y.; Wang, R.; An, Q.; Su, X.; Li, C.; Shen, S.; Huo, G. The F···H Hydrogen Bonding Effect on the Dynamic Mechanical and Shape-Memory Properties of a Fluorine-Containing Polybenzoxazine. *Macromol. Chem. Phys.* **2017**, *218*, 1700079.

(S83) Li, J.; Liu, T.; Pan, Y.; Xia, S.; Zheng, Z.; Ding, X.; Peng, Y. A Versatile Polymer Co-Network with Broadened Glass Transition Showing Adjustable Multiple-Shape Memory Effect. *Macromol. Chem. Phys.* **2012**, *213*, 2246-2252.

(S84) Peterson, G. I.; Childers, E. P.; Li, H.; Dobrynin, A. V.; Becker, M. L. Tunable Shape Memory Polymers from α-Amino Acid-Based Poly(ester urea)s. *Macromolecules* **2017**, *50*, 4300-4308.

(S85) Yu, K.; Dunn, M. L.; Qi, H. J. Digital Manufacture of Shape Changing Components. *Extreme Mechan. Lett.* **2015**, *4*, 9-17.

(S86) Samuel, C.; Barrau, S.; Lefebvre, J. M.; Raquez, J. M.; Dubois, P. Designing Multiple-Shape Memory Polymers with Miscible Polymer Blends: Evidence and Origins of a Triple-Shape Memory Effect for Miscible PLLA/PMMA Blends. *Macromolecules* **2014**, *47*, 6791-6803.

(S87) Ware, T.; Hearon, K.; Lonnecker, A.; Wooley, K. L.; Maitland, D. J.; Voit, W. Triple-Shape Memory Polymers Based on Self-Complementary Hydrogen Bonding. *Macromolecules* **2012**, *45*, 1062-1069.

(S88) Xiao, R.; Guo, J.; Safranski, D. L.; Nguyen, T. D. Solvent-Driven Temperature Memory and Multiple Shape Memory Effects. *Soft Matter* **2015**, *11*, 3977-3985.

(S89) Zheng, N.; Hou, J.; Xu, Y.; Fang, Z.; Zou, W.; Zhao, Q.; Xie, T. Catalyst-Free Thermoset Polyurethane with Permanent Shape Reconfigurability and Highly Tunable Triple-Shape Memory Performance. *ACS Macro Lett.* **2017**, *6*, 326-330.

(S90) Xie, T. Tunable Polymer Multi-Shape Memory Effect. *Nature* **2010**, *464* , 267-270.

(S91) Yang, Z.; Wang, Q.; Wang, T. Tunable Triple-Shape Memory Binary Mixtures with High Transition Temperature and Robust Mechanical Properties. *Macromol. Chem. Phys.* **2016**, *217*, 1305-1313.

(S92) Dong, Y.; Xia, H.; Zhu, Y.; Ni, Q.-Q.; Fu, Y. Effect of Epoxy-Graft-Polyoxyethylene Octyl Phenyl Ether on Preparation, Mechanical Properties and Triple-Shape Memory Effect of Carbon Nanotube/Water-Borne Epoxy Nanocomposites. *Compos. Sci. Technol.* **2015**, *120*, 17-25.

(S93) Zhang, X.; Tang, Z.; Guo, B.; Zhang, L. Enabling Design of Advanced Elastomer with Bioinspired Metal-Oxygen Coordination. *ACS Appl. Mater. Interfaces* **2016**, *8*, 32520-32527.

(S94) Zhang, Q.; Wei, H.; Liu, Y.; Leng, J.; Du, S. Triple-Shape Memory Effects of Bismaleimide Based Thermosetting Polymer Networks Prepared via Heterogeneous Crosslinking Structures. *RSC Adv.* **2016**, *6*, 10233-10241.

(S95) Zhang, Y.; Li, W.; Wu, R.; Wang, W. PU/PMMA Composites Synthesized by Reaction-Induced Phase Separation: a General Approach to Achieve a Shape Memory Effect. *RSC Adv.* **2017**, *7*, 33701-33707.

(S96) Zhang, F.; Zhang, Z.; Liu, Y.; Lu, H.; Leng, J. The Quintuple-Shape Memory Effect in Electrospun Nanofiber Membranes. *Smart Mater. Struct.* **2013**, *22*, 085020.

(S97) Wang, K.; Jia, Y.-G.; Zhu, X. X. Biocompound-Based Multiple Shape Memory Polymers Reinforced by Photo-Cross-Linking. *ACS Biomater. Sci. Eng.* **2015**, *1*, 855-863.

(S98) Zhuo, S.; Zhang, G.; Feng, X.; Jiang, H.; Shi, J.; Liu, H.; Li, H. Multiple Shape Memory Polymers for Self-Deployable Device. *RSC Adv.* **2016**, *6*, 50581-50586.

(S99) Zou, F.; Chen, H.; Fu, S.; Chen, S. Shape Memory Materials Based on Adamantane-Containing Polyurethanes. *RSC Adv.* **2018**, *8*, 25584-25591.

(S100) Chen, S.; Mo, F.; Stadler, F. J.; Chen, S.; Ge, Z.; Zhuo, H. Development of Zwitterionic Copolymers with Multi-Shape Memory Effects and Moisture-Sensitive Shape Memory Effects. *J. Mater. Chem. B* **2015**, *3*, 6645-6655.

(S101) Chen, S.; Mei, Z.; Ren, H.; Zhuo, H.; Liu, J.; Ge, Z. Pyridine Type Zwitterionic Polyurethane with Both Multi-Shape Memory Effect and

Moisture-Sensitive Shape Memory Effect for Smart Biomedical Application. *Polym. Chem.* **2016**, *7*, 5773-5782.

(S102) Zhuo, H.; Mei, Z.; Chen, H.; Chen, S. Chemically-Crosslinked Zwitterionic Polyurethanes with Excellent Thermally-Induced Multi-Shape Memory Effect and Moisture-Induced Shape Memory Effect. *Polymer* **2018**, *148*, 119-126.

(S103) Nöchel, U.; Kumar, U. N.; Wang, K.; Kratz, K.; Behl, M.; Lendlein, A. Triple-Shape Effect with Adjustable Switching Temperatures in Crosslinked Poly[ethylene-co-(vinyl acetate)]. *Macromol. Chem. Phys.* **2014**, *215*, 2446-2456.

(S104) Bai, Y.; Jiang, C.; Wang, Q.; Wang, T. Multi-Shape-Memory Property Study of Novel Poly(ε-caprolactone)/Ethyl Cellulose Polymer Networks. *Macromol. Chem. Phys.* **2013**, *214*, 2465-2472.

(S105) Hoeher, R.; Raidt, T.; Krumm, C.; Meuris, M.; Katzenberg, F.; Tiller, J. C. Tunable Multiple-Shape Memory Polyethylene Blends. *Macromol. Chem. Phys.* **2013**, *214*, 2725-2732.

(S106) Zhang, Q.; Song, S.; Feng, J.; Wu, P. A New Strategy to Prepare Polymer Composites with Versatile Shape Memory Properties. *J. Mater. Chem.* **2012**, *22*, 24776-24782.

(S107) Yang, X.; Wang, L.; Wang, W.; Chen, H.; Yang, G.; Zhou, S. Triple Shape Memory Effect of Star-Shaped Polyurethane. *ACS Appl. Mater. Interfaces* **2014**, *6*, 6545-6554.

(S108) Wang, L.; Yang, X.; Chen, H.; Yang, G.; Gong, T.; Li, W.; Zhou, S. Multi-Stimuli Sensitive Shape Memory Poly(vinyl alcohol)-Graft-Polyurethane. *Polym. Chem.* **2013**, *4*, 4461-4468.

(S109) Ahn, S.-k.; Kasi, R. M. Exploiting Microphase-Separated Morphologies of Side-Chain Liquid Crystalline Polymer Networks for Triple Shape Memory Properties. *Adv. Funct. Mater.* **2011**, *21*, 4543-4549.

(S110) Ahn, S.-k.; Deshmukh, P.; Kasi, R. M. Shape Memory Behavior of Side-Chain Liquid Crystalline Polymer Networks Triggered by Dual Transition Temperatures. *Macromolecules* **2010**, *43*, 7330-7340.

(S111) Li, M. Q.; Song, F.; Chen, L.; Wang, X. L.; Wang, Y. Z. Flexible Material Based on Poly(lactic acid) and Liquid Crystal with Multishape Memory Effects. *ACS Sustain. Chem. Eng.* **2016**, *4*, 3820-3829.

(S112) Wen, Z. B.; Liu, D.; Li, X. Y.; Zhu, C. H.; Shao, R. F.; Visvanathan, R.; Clark, N. A.; Yang, K. K.; Wang, Y. Z. Fabrication of Liquid Crystalline Polyurethane Networks with a Pendant Azobenzene Group to Access Thermal/Photoresponsive Shape-Memory Effects. *ACS Appl. Mater. Interfaces* **2017,** *9*, 24947-24954.

(S113) Wen, Z.; Zhang, T.; Hui, Y.; Wang, W.; Yang, K.; Zhou, Q.; Wang, Y. Elaborate Fabrication of Well-Defined Side-Chain Liquid Crystalline Polyurethane Networks with Triple-Shape Memory Capacity. *J. Mater. Chem. A* **2015,** *3*, 13435-13444.

(S114) Fu, S.; Zhang, H.; Zhao, Y. Optically and Thermally Activated Shape Memory Supramolecular Liquid Crystalline Polymers. *J. Mater. Chem. C* **2016,** *4*, 4946-4953.

(S115) Torbati, A. H.; Nejad, H. B.; Ponce, M.; Sutton, J. P.; Mather, P. T. Properties of Triple Shape Memory Composites Prepared via Polymerization-Induced Phase Separation. *Soft Matter* **2014,** *10*, 3112-3121.

(S116) Bellin, I.; Kelch, S.; Langer, R.; Lendlein, A. Polymeric Triple-Shape Materials. *Proc. Natl. Acad. Sci. USA.* **2006,** *103*, 18043-18047.

(S117) Razzaq, M. Y.; Behl, M.; Kratz, K.; Lendlein, A. Triple-Shape Effect in Polymer-Based Composites by Cleverly Matching Geometry of Active Component with Heating Method. *Adv. Mater.* **2013,** *25*, 5514-5518.

(S118) Bai, Y.; Zhang, X.; Wang, Q.; Wang, T. A Tough Shape Memory Polymer with Triple-Shape Memory and Two-Way Shape Memory Properties. *J. Mater. Chem. A* **2014,** *2*, 4771-4778.

(S119) Podgorski, M.; Wang, C.; Bowman, C. N. Multiple Shape Memory Polymers Based on Laminates Formed from Thiol-Click Chemistry Based Polymerizations. *Soft Matter* **2015,** *11*, 6852-6858.

(S120) Zhang, Q.; Hua, W.; Feng, J. A Facile Strategy to Fabricate Multishape Memory Polymers with Controllable Mechanical Properties. *Macromol. Rapid Commun.* **2016,** *37*, 1262-1267.

(S121) Yu, L.; Wang, Q.; Sun, J.; Li, C.; Zou, C.; He, Z.; Wang, Z.; Zhou, L.; Zhang, L.; Yang, H. Multi-Shape-Memory Effects in a Wavelength-Selective Multicomposite. *J. Mater. Chem. A* **2015,** *3*, 13953-13961.

(S122) Li, J.; Liu, T.; Xia, S.; Pan, Y.; Zheng, Z.; Ding, X.; Peng, Y. A Versatile Approach to Achieve Quintuple-Shape Memory Effect by Semi-Interpenetrating Polymer Networks Containing Broadened Glass Transition and Crystalline Segments. *J. Mater. Chem.* **2011,** *21*, 12213-12217.

(S123) Kolesov, I. S.; Radusch, H. J. Multiple Shape-Memory Behavior and Thermal-Mechanical Properties of Peroxide Cross-Linked Blends of Linear and Short-Chain Branched Polyethylenes. *Express Polym. Lett.* **2008,** *2*, 461-473.

(S124) Radusch, H.-J.; Kolesov, I.; Gohs, U.; Heinrich, G. Multiple Shape-Memory Behavior of Polyethylene/Polycyclooctene Blends Cross-Linked by Electron Irradiation. *Macromol. Mater. Eng.* **2012,** *297*, 1225-1234.

(S125) Song, Q.; Chen, H.; Zhou, S.; Zhao, K.; Wang, B.; Hu, P. Thermo- and pH-Sensitive Shape Memory Polyurethane Containing Carboxyl Groups. *Polym. Chem.* **2016,** *7*, 1739-1746.

(S126) Kuang, X.; Liu, G.; Dong, X.; Wang, D. Triple-Shape Memory Epoxy Based on Diels–Alder Adduct Molecular Switch. *Polymer* **2016,** *84*, 1-9.

(S127) Wu, Y.; Hu, J.; Zhang, C.; Han, J.; Wang, Y.; Kumar, B. A Facile Approach to Fabricate a UV/Heat Dual-Responsive Triple Shape Memory Polymer. *J. Mater. Chem. A* **2015,** *3*, 97-100.

(S128) He, Z.; Satarkar, N.; Xie, T.; Cheng, Y. T.; Hilt, J. Z. Remote Controlled Multishape Polymer Nanocomposites with Selective Radiofrequency Actuations. *Adv. Mater.* **2011,** *23*, 3192-3196.

(S129) Xie, H.; Deng, X. Y.; Cheng, C. Y.; Yang, K. K.; Wang, Y. Z. New Strategy to Access Dual-Stimuli-Responsive Triple-Shape-Memory Effect in a Non-overlapping Pattern. *Macromol. Rapid Commun.* **2017,** *38*, 1600664.

(S130) Zhou, L.; Liu, Q.; Lv, X.; Gao, L.; Fang, S.; Yu, H. Photoinduced Triple Shape Memory Polyurethane Enabled by Doping with Azobenzene and GO. *J. Mater. Chem. C* **2016,** *4*, 9993-9997.

(S131) Dreyfuss, P. *Poly(tetrahydrofuran)*. Gordon and Breach Science Publishers: New York, **1982**, 157.

(S132) Crescenzi, V.; Manzini, G.; Calzolari, G.; Borri, C. Thermodynamics of Fusion of Poly-β-propiolactone and Poly-ε-caprolactone. Comparative Analysis of the

Melting of Aliphatic Polylactone and Polyester Chains. *Eur. Polym. J.* **1972**, *8*, 449-463.